PRECIPITATION IN THE MEDITERRANEAN REGION OBSERVED WITH TRMM MICROWAVE DATA

Martina Kästner and Jörg Steinwagner

Deutsches Zentrum für Luft- und Raumfahrt (DLR), Deutsches Fernerkundungsdatenzentrum (DFD), Oberpfaffenhofen, D-82234 Wessling, P.O. Box 1116, Germany

ABSTRACT

Different satellite rain estimations based on microwave (MW), infrared (IR) or combined MW-IR techniques and contrasts them with the mesoscale Bologna local area model (BOLAM) rain analysis or the network based gauge data from the Global Precipitation Climate Centre (GPCC) for a period from 08 to 13 November 2001 over the western Mediterranean Sea during a severe weather event, which resulted in a disastrous flood in Algeria. The PR Adjusted TMI Estimation of Rainfall (PATER) and frequency difference algorithm (FDA) are applied to MW TRMM data, the neural rain estimator (NRE) uses geostationary IR Meteosat data and the combined NRL Turk algorithm uses both, MW data from low orbiting satellites and IR data from a geostationary orbit. The unique gridded data provide an effective basis to compare instantaneous space measurements with different algorithms.

Validation results indicate that there is generally a better performance for heavy rain than for weak rain. Both MW algorithms, PATER and FDA, perform rather similarly whereas PATER is applicable exclusively over the ocean and shows some rain detection problems due to thick aerosol loads originating from the desert. The BOLAM model performs rather well in this case study, only a small location error of a heavy rain area was analyzed. The IR based techniques have the advantage of a high temporal revisit but both algorithms, NRL and NRE, have problems with identifying the correct rainy areas compared to MW results. Overall, the results suggest combining both advantages, the well-known rain physics of the MW channels with the high temporal resolution of IR algorithms, to retrieve precipitation operationally from satellite data.

1. INTRODUCTION

Various climate models predict a decrease of precipitation in the future over many parts of the subtropics, particularly in the winter (Bolle, 2003). Therefore, it is essential to have not only climatological data from land but also from over the seas. Remote areas are not covered by conventional observation networks, they can now be continuously monitored by low orbiting and geostationary satellites. The first satellite rain retrievals in both the IR and the MW spectra date back to the 1970s, some recent works are Turk et al. (2000), Bauer (2000, 2001a+b), Levizzani et al. (2001), Grose et al. (2002), Oh et al. (2002), Tapiador (2002) and Kidd et al. (2003) among others. A cross-comparison of TRMM and GPCP rainfall data sets are described in Adler et al. (2002).

The evaluation of passive MW precipitation algorithms which are directly linked to the 3-D structure of the precipitating system use measurements from different sensors on different satellites, like SSM/I on DMSP, TMI/PR on TRMM, or AMSU on NOAA. Passive MW techniques perform much better over the oceans than over land. The MW techniques are directly related to the hydrometeors through scattering and emission, but the low earth orbits and less frequent coverage hinders tracking of developing severe storms. While the daily course of precipitation is not easily obtained from TRMM data, IR-based techniques from geostationary satellites have been widely used due to the high revisit period. However, they have an inherent weakness regarding the physical relation between cloud top temperatures and underlying rain rate. Further, the rain characteristics vary with different climate regimes, hence, any developed method has to be validated against appropriate in situ measurements taken over the region of interest.

An inter-comparison of PMW and/or IR based algorithms with BOLAM model data and GPCC gauge measurements in different spatial resolutions is performed for the Algerian flood in early November 2001. Although the validity of the results obtained is restricted to the case studies some general information could be extracted.

2. DATA

The validation of various rain algorithms is performed for a severe weather event between 08 and 12 November 2001 on the Algerian coast and the Balearic Islands. The synoptic situation was characterised by strong surface winds and heavy rainfall. An intense upper-level trough pushed far to the south of Europe where a cut-off low developed. The METEOSAT-7 IR image (Figure 2) shows the clouds with heavy rainfall on the Algerian coast. The rainfall started on late 9 November and ended the next day at about noon on 10 November 2001, when 150 litres per m² within six hours were observed. Together with the cut-off low process heavy thunderstorms developed in a cyclogenesis over the Balearic Islands the next day. The precipitation was reported to be greater than 400 mm over two days, with a maximum of 68 litres per m² in six hours (Thomas et al., 2003).

Two processes intensified the convective development: 1) the cold maritime arctic air that crossed over the still 18°C warm Mediterranean Sea where it picked up moisture, destabilised it, and met initially maritime subtropic air and, 2) the strong surface winds blowing against the high mountains along the African coast (above 2300 m) caused intense orographic rainfall which led to the flooding disaster in Algiers with more than 750 deaths.

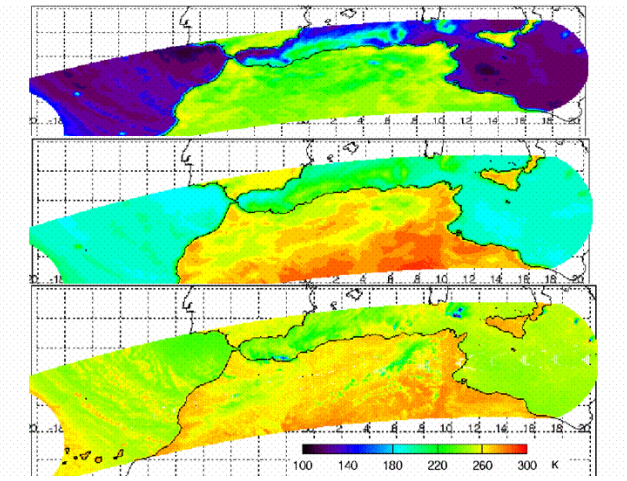

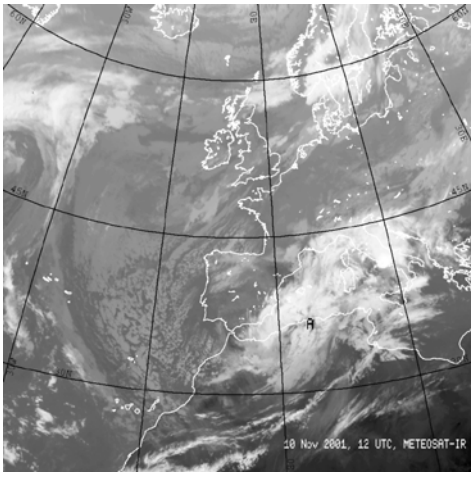

Figure 1 (left): TRMM TMI brightness temperatures for 19h (top), 19v (mid) and 85v (bottom) GHz channels (v = vertical, h = horizontal polarization), orbit time: 10 November 2001, 00:25 UTC.

Figure 2 (right): METEOSAT-7 IR, 10 November 2001, 12 UTC. A = Algiers.

Input data for PMW algorithms (PATER, FDA) are the TMI brightness temperatures (TB) of nine channels (10.7v,h, 19.4v,h, 21.3v, 37.0v,h, 85.5v,h GHz) with varying resolutions from 70 to 6 km. Figure 1 shows differences of emission over water and over land for both polarizations and for three different TMI channels. Over water, the rainy areas appear to be warmer than their surroundings, while over land they appear to be colder due to the high MW emission of land.

The applied rain retrievals and rain data are briefly described:

The BOLAM (Bologna local area model) is a hydrostatic, primitive equation, gridpoint model in σ coordinates, using horizontal wind components, potential temperature, specific humidity and surface pressure as basic dependent variables. The initial and boundary conditions are obtained from the ECMWF 6-hourly analyses.

The frequency difference algorithm (FDA) of Ch. Kidd uses the 19v and 19h GHz channels and relates it to the rain rate (RR), as described in Ebert et al. (1996). It is a PMW satellite rain algorithm that is operationally applied to TRMM as well as SSM/I orbit data.

Independent one-degree-daily (1DD) data from the Global Precipitation Climate Centre (GPCC) base on recordings of the very dense rain gauge network in Europe, the SYNOP reports are automatically checked and corrected for systematic measuring errors (Rudolf et al., 1996).

The neural Rain Estimator (NRE) is an operational rapid update IR-based algorithm to diagnose half-hourly near-surface rainfall. It is an empirical technique suited for acquisitions from geostationary satellites. It uses some relevant features of the cloud top evolution and structure and information from a NWP model.

The basic strategy for the NRL (Naval Research Laboratory) blended technique (Turk et al., 2000) draws upon the probability matching methods developed in the radar meteorology field for specific 'tuned' Z-R relations. Time- and space-coincident IR and MW pixels are collected from different satellites and used to produce dynamically-updated TB-RR lookup tables.

The over-ocean satellite rainfall algorithm PATER is a physical algorithm that uses only two empirical orthogonal functions instead of the nine TBs from the TMI channels. The retrieval database is generated from several 3-D cloud model simulations including the melting layer (Bauer, 2001a). The algorithm (Bauer et al., 2001b) has a stand-alone PMW component based on TRMM TMI (1B11) data and an optionally carefully co-located calibration with PR (2A25) data (~5 km) upscaled to the lower TMI spatial resolution for the 10 GHz (~50 km).

3. METHOD OF ANALYSIS

In a pre-study the rain rates (RR) of the PATER over-ocean algorithm were merged from three TRMM overflights daily and then upscaled to a 1°x1° grid for comparison with the independent RR gauge data from the 1DD GPCC data.

For the main study a common area, period, grid, and format were essential for combining data sets with different temporal or spatial resolutions sometimes describing different physical observables. All subsequent tasks like calibration, sampling, or error analysis needed a common grid that allowed an equivalent evaluation. For the joint effort of validation and inter-comparison of several rain algorithms applied in the scope of the EURAINSAT project, continuous and categorial statistics were used according to Ebert et al. (1996, 1998).

The Algerian severe weather event was used as a common case study for an inter-comparison of PMW, IR, combined MW/IR rainfall algorithms and the BOLAM model. The common area extended from 15 W to 20 E and from 30 to 60 N; with a common period from 09 to 11 November 2001; and with RR data re-sampled into a 0.25°x0.25° lat-lon grid (~28 km). TRMM and IRE data did not both consistently cover the complete common area, therefore, the subsequent comparison was conducted only over the available common area. The temporal coincidence was optimal for the different PMW algorithms, because PATER and FDA have the same TRMM database, otherwise the temporal window was better than +/-15 min for comparisons with IR (NRL, NRE) and in most cases better than +/-90 minutes for comparisons with the independent model data, which have a 3-hourly temporal resolution. Comparisons were made for single orbits as well as for merged data within 3-h periods.

4. RESULTS

4.1. Intercomparison - PATER and other rain retrievals on a 0.25° grid

A validation study of the satellite rainfall estimations has been performed for the Algerian case using independent inter-comparison of different rainfall retrievals, including pure PMW, pure IR, combined MW/IR techniques and model results using BOLAM before nudging with satellite rainfall data. Both PMW algorithms, PATER and FDA, rely on the same TMI orbit data and so it was expected that their comparison would result in a rather similar rainfall region and intensity. Both algorithms are assessed to be of equal quality in this heavy rainfall event, considering that the PATER algorithm is restricted to ocean surfaces and to rain events above 1mm/h. The most successful comparison of pure PMW with other techniques was in this case the

BOLAM model followed by the NRL blended MW/IR technique both of which performed better than the pure IR technique.

The results of the inter-comparison of different rain retrievals are given for visual inspection for a single date (10 Nov. 2001, 03 UTC) (Figures 3 to 5). A complete analysis of the categorical statistics of all possible combinations of the above described algorithms within the period 08 to 13 November 2001 is given in Table 1.

Figures 3 and 4 show three areas of heavy rainfall, one west of the Canary Islands, the biggest one is around Algiers, and one southeast of Sardinia. The three rain areas coincide very well with results of both MW algorithms. Even the rain intensities are similar except for the Sardinia area. FDA works over land and ocean, PATER exclusively over ocean and for rainfall rates above 1mm/h. The low rain rates erroneously detected over the sea south of Sicily (Figure 3) are attributed to strong desert aerosol also detected as aerosol fallout in Rome the next day. The rainy speckles over the Atlantic are due to cumulus convective showers within the cold air.

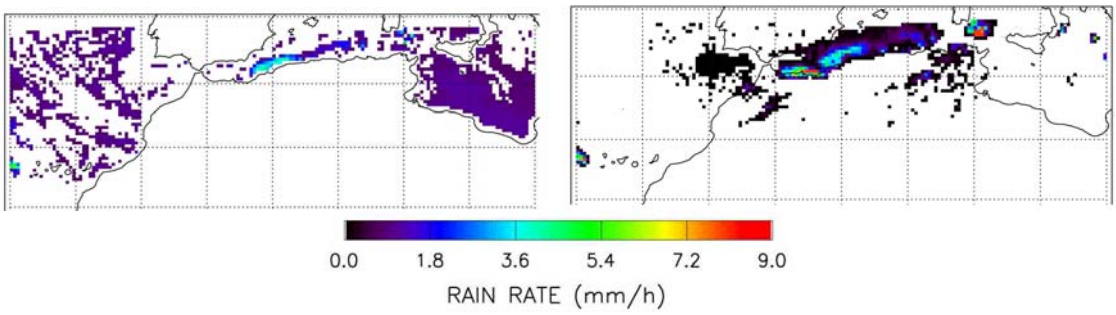

Figure 3 (left): PATER algor. – MW ; 10 November 2001, TMI orbit 22741+22742, 00:25+02:10 UTC.

Figure 4 (right): same as Fig.3, but FDA algor. – PMW

Compared to the PMW techniques, the BOLAM model rainfall (before nudging) shows wide agreement of the strong rain bands (Figure 5 upper left). The rainfall intensities were rather similar; only the position of the rainfall had an error for the Sardinia area. On the other hand, the shower pattern over the Atlantic is not well matched and there are too many areas with light rain. The two IR-based algorithms, NRL and NRE (Figure 5**),** give heavy rain areas over the Mediterranean Sea, but not at the correct position. The Algerian coast, where the maximum precipitation fell, is hardly classified as a heavy rain area. The combined MW/IR NRL algorithm shows a much better performance than the IR algorithm NRE alone.

Overall it seems to be worthwhile to combine the high temporal resolution of IR with the better rainfall identification performance of MW techniques for monitoring purposes. The NRL algorithm or the now available TRMM 3B42RT products belong to this category. The low MW pixel resolution makes a 0.25° lat-lon grid appropriate, but better spatial resolution is desired by the users.

The event occurrences of the contingency table for comparisons within the time period 09 to 11 November 2001 consider the above mentioned temporal windows (Table 1). The number of compared pairs (N) differs for each algorithm pair; thus, the occurrences are given in percent of each N for better comparison between the cases, the maxima (hits) or minima (false alarms) are italicized. The following abbreviations are used: B = BOLAM, F = FDA, P = PATER.

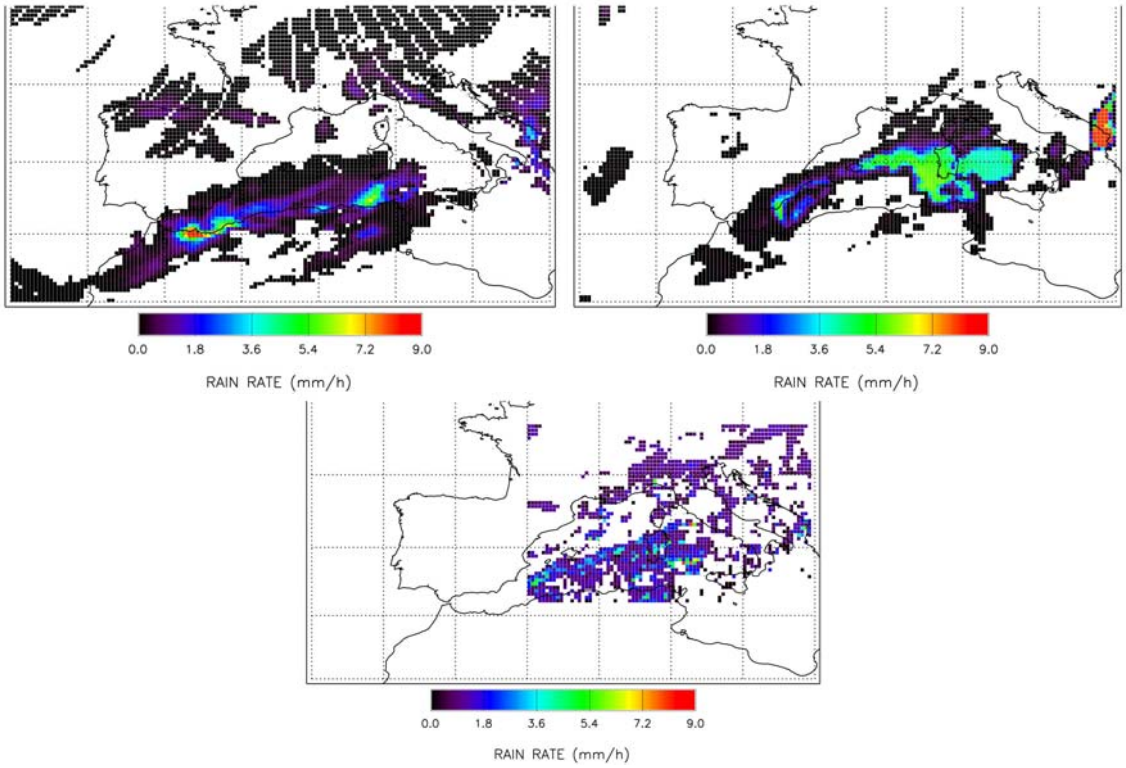

Figure 5: 10 November 2001, 03 UTC: upper left: BOLAM – model, upper right: NRL Turk algorithm – combined IR-MW, bottom: NRE (neural rain estimator) – IR

The accuracy of all inter-comparisons is measured in terms of Heidke skill score (HSS), and ranges from 0.61 (BOLAM vs. NRE), to respectable 0.78 (BOLAM vs. FDA), to optimal 0.82 (PATER vs. FDA). No bias between the data sets is indicated when the bias value is unity, thus, PATER and NRL have only a small bias, while again PATER performs best when compared with FDA. Note that even in this heavy rain event only 10% of the gridded pixels are hits (rain/rain), whereas the majority (62%) is correct negatives (no-rain/no-rain), thus, the correct negatives dominate the statistics.

	Compared pairs	hit	miss	false alarm	correct negative	Heidke skill score	bias score
	N = 100%	*%*	*%*	*%*	*%*	*best = 1*	*best = 1*
P vs. B	8.346	4.9	21.1	11.9	62.2	0.67	0.65
P vs. NRE	2.595	7.2	16.6	20.0	56.1	0.63	1.14
P vs. NRL	14.619	3.3	14.3	15.2	67.2	0.70	1.05
B vs. NRE	3.774	*22.3*	10.0	28.6	39.2	0.61	1.58
B vs. NRL	13.880	9.9	13.3	10.9	65.9	0.76	0.89
NRE vs. NRL	6.320	20.6	15.6	11.1	52.6	0.73	0.88
F vs. P	3.353	2.5	*8.9*	8.9	*79.7*	*0.82*	*1.01*
F vs. B	6.128	11.2	18.3	4.2	66.3	0.78	0.52
F vs. NRL	7.142	5.0	15.2	*3.9*	75.9	0.81	0.44
F vs. NRE	931	12.5	23.3	7.8	56.3	0.69	0.57
total	67.088	9.9	15.7	12.3	62.1	0.72	0.87

Table 1: Categorial statistics for different satellite rain retrievals.

4.2. Monthly mean precipitation over the Mediterranean Region

Various climate models predict a decrease of precipitation for future changes over many parts of the subtropics, particularly in the winter (Bolle (ed.), 2003). Therefore, it is essential to have not only climatological data from land but also from over the seas. Based on a quasi operational data production with the PATER precipitation algorithm that combines TMI with PR TRMM data, a series of data sets (August 2002 till June 2003) has been processed with special interest on the Eastern North Atlantic and the Mediterranean Sea in a high spatial resolution of ~28 km. The daily course of precipitation is not easily obtained from TRMM data because of the low orbit, but daily, pentade and monthly means of gridded PATER rainfall rates are re-sampled into a common grid for inter-comparison with other techniques.

The geographical distribution of monthly means of precipitation over water (excluding the coastlines) is shown in Figure 6 for a) November 2002, b) January 2003, c) March 2003 and d) May 2003. During the winter rainy season the rain intensity steadily increases from October to March and then quickly drops to the lower May values. Note, that the rain rate is given in mm/h is calculated from only three TRMM orbits per day, therefore the maximum value of 1.2 on the linear scale corresponds to 110 mm precipitation per month. The distribution of precipitation shows an obvious east-west-gradient within the Atlantic to the coast of Africa, especially in January (Figure 6 b) and May (Figure 6 d). Further, the data set shows the gradient to the north over the Atlantic, especially in November (Figure 6 a).

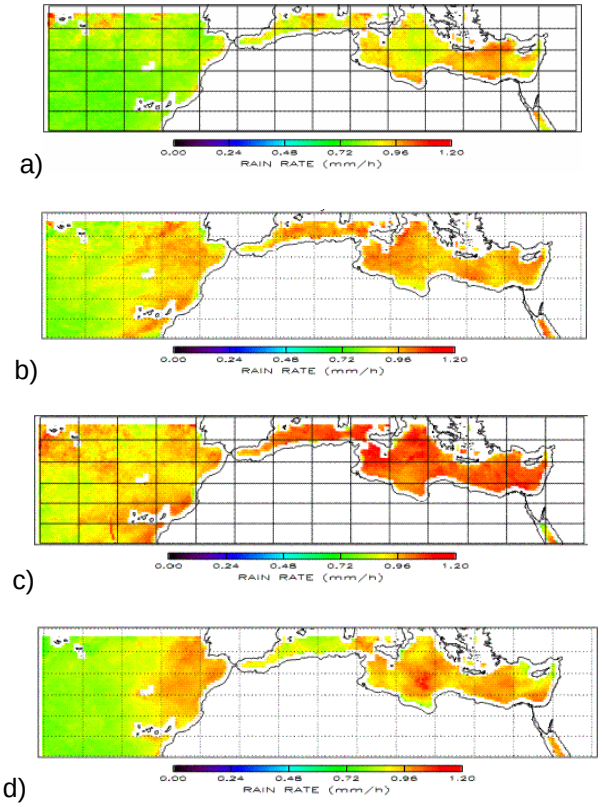

Figure 6: PATER retrieval: Geographical distribution of precipitation in the winter season 2002/2003, a) November 2002, b) January 2003, c) March 2003, d) May 2003, 0.2° spatial resolution.

5. CONCLUSION AND DISCUSSION

A heavy rainfall situation was selected for a validation analysis of different satellite rainfall algorithms representing MW, IR or combined MW/IR retrievals and the BOLAM model. The rainfall data were gridded on a 0.25°-grid in a common area over Western Europe, categorical statistics are used.

Special interest was laid on the PATER algorithm that uses TRMM active and passive MW data. The PATER retrieval is crucially dependent on the forward 3-D cloud model calculations. There is a need for better and more comprehensive cloud models that cover the whole spectrum of natural clouds, particularly clouds with moderate and light rain and snow.

In this case study the PMW techniques performed better than IR techniques. Overall, the results suggest combining both advantages, the well-known rain physics of the MW channels with the high temporal resolution of IR algorithms, to retrieve precipitation from satellite data.

The correlation coefficient r is often used in comparison tasks. It has already been shown that r is dependent on the choice of the grid size (Turk et al., 2002). In this study the maximum r is reached for both PMW techniques, namely r is 0.88 for PATER vs. FDA (orbit 22741, 0.25° grid).

The accuracy is measured in terms of Heidke skill score, which is a combination of hits, false alarms, misses and correct negatives. HSS is truly dependent on the threshold RR-min, discriminating rain from no-rain pixels. Figure 7 results from varying the minimum detectable rain rate (RR-min) for the rain algorithm pair PATER vs. FDA. The event occurrences for each category are given on the y-axis. For RR-min = 1 mm/h, false alarms (red) and misses (blue) are of the same order, which means that in this case the algorithms are unbiased. The impact of RR-min on the accuracy is evident; the strong increase of HSS from 0.3 to 0.8 for RR-min greater than 0.7 mm/h indicates that higher rain rates are more accurately detected than low ones. This implies that not only the chosen grid size but also the problem on where the rain/no-rain threshold is set is inherently associated with the accuracy problem.

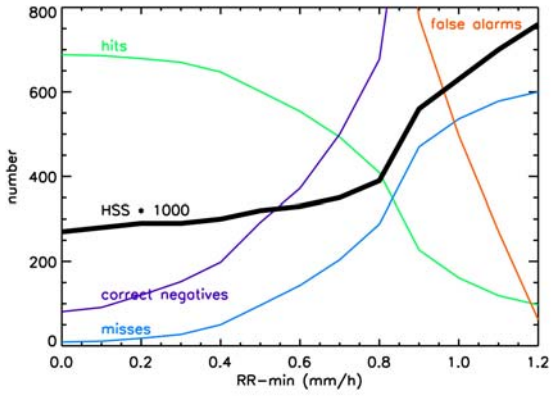

Figure 7: Comparison of rainfall retrievals PATER vs. FDA. The accuracy given by HSS*1000 (thick) depends on the rain/no-rain threshold RR-min

As the statistics are dominated by the correct negatives and not by the hits, maybe the use of entity-based methods, like CRA (contiguous rain area) verification give further insight into algorithm performances (Ebert, 2000).

6. ACKNOWLEDGEMENT

This research is funded in by the EURAINSAT project, a shared-cost project (contract EVG1-2000-00030), co-funded by the Research DG of the European Commission within the RTD activities of a generic nature of the Environment and Sustainable Development sub-programme 5th Framework Programme).

7. REFERENCES

ADLER R.F., Huffman G., Bolvin D. TRMM and GPCP initial cross-comparison. *GEWEX News* 2002, 12 (Nov): 5-6.

BAUER P, Burose D, Schulz J. Rain detection over land surfaces using passive microwave satellite data. ECMWF Tech. Memo. No. 330, Reading, England, 2000.

BAUER P. Over–Ocean Rainfall Retrieval from Multisensor Data of the Tropical Rainfall Measuring Mission. Part I: Design and Evaluation of Inversion Databases. *J. Atmos. Oceanic Technol* 2001a;, 18: 1315-1330.

BAUER P., Amayenc P., Kummerow C.D., Smith E.A. Over–Ocean Rainfall Retrieval from Multisensor Data of the Tropical Rainfall Measuring Mission. Part II: Algorithm Implementation. *J. Atmos. Oceanic Technol.* 2001b; 18: 1838-1855.

BOLLE, H.-J. (ed.), *Mediterranean Climate – Variablility and Trends*. Berlin, Springer, 372 pp, 2003.

BUZZI A., D'Isidoro M., Davolio S. A case study of an orographic cyclone formation south of the Alps during the MAP-SOP. *Q. J. R. Meteorol. Soc.* 2003, 129: 1795-1818.

EBERT, E.E. Results of the 3rd Algorithm Intercomparisons Project (AIP-3) of the Global Precipitation Climatology Project (GPCP). Revision I. Bureau of Meteorology Research Centre, Melbourne, Australia, 199 pp., 1996.

EBERT E.E., Manton M.J. Performance of Satellite Rainfall Estimation Algorithms during TOGA COARE. *J. Atmos. Sci.* 1998; 55: 1537-1557.

EBERT E.E., McBride J.L. Verification of precipitation in weather systems: determination of systematic errors. *J. Hydrol.* 2000; 239: 179-202.

GROSE A., Smith E.A., Chung H.-S., Ou M.L., Sohn B.J., Turk F.J. Possibilities and limitations for QPF using nowcasting methods with infrared geosynchronous satellite imagery. *J. Appl. Meteor.* 2002; 41: 763-785.

KÄSTNER M. Inter-comparison of precipitation estimations using TRMM microwave data and independent data. In: Proc. 3rd GPM Workshop - Consolidating the Concept, Noordwijk, The Netherlands, 24-26 June 2003, AP-5, 2003.

KIDD C., Kniveton D., Todd M., Bellerby, T. Satellite rainfall estimation using a combined passive microwave and infrared algorithm. *J. Hydrometeorology* 2003; 4: 1088-1104.

OH H.J., Sohn B.J., Smith E.A., Turk F.J., Seo A.S., Chung H.S. Validating infrared-based rainfall retrieval algorithms with 1-minute spatially dense raingauge measurements over the Korean peninsula. *Meteor. Atmos. Physics* 2002; 81: 273-287.

LEVIZZANI V., Schmetz J., Lutz H.J., Kerkmann J., Alberoni P. P., Cervino M. Precipitation estimations from geostationary orbit and prospects for METEOSAT Second Generation. *Meteorol. Appl.* 2001; 8: 23–41.

RUDOLF, B., H. Hauschild, M. Reiß,U. Schneider. Beiträge zum Weltzentrum für Niederschlagsklimatologie – Contributions to the Global Precipitation Climatology Centre. *Meteorologische Zeitschrift N. F.* 1992, 1: 7-84.

TAPIADOR, F. A new algorithm to generate global rainfall rates from satellite infrared imagery. *Revista de Teledeteccion* 2002, 18:57-61.

THOMAS W., Baier F., Erbertseder T., Kästner M. Analysis of the Algerian severe weather event in November 2001 and its impact on ozone and nitrogen dioxide distributions. *Tellus B*, 2003; 55B: 993-1006.

TURK FJ, Hawkins J, Smith EA, Marzano S, Mugnai A, Levizzani V. Combining SSM/I, TRMM and infrared geostationary satellite data in a near real-time fashion for rapid precipitation updates: advantages and limitations. In: Proc. The 2000 EUMETSAT Meteorological Satellite Data Users' Meeting, Bologna, Italy, 29 May – 2 June 2000; EUM P 29: 452-459.

TURK FJ, Ebert EE, Oh HJ, Sohn BJ, Levizzani V, Smith EA, Ferraro R. Validation of an operational global precipitation analysis at short time scales. In: Proc. 1st Workshop Intern. Precip. Working Group (IPWG), Madrid, Spain, 23-27 Sept. 2002.